Thermochimica Acta, 199 (1992) 35–43
Elsevier Science Publishers B.V., Amsterdam

The specific heat of $[N(CH_3)_4]_2ZnBr_4$ around the ferro-paraelastic phase transition by adiabatic calorimetry [1]

J.M. Igartua [a], I. Ruiz-Larrea [a], J. Zubillaga [a], A. López-Echarri [a] and M. Couzi [b]

[a] *Departamento de Física de la Materia Condensada, Facultad de Ciencias, U.P.V. / E.H.U., 48080 Bilbao (Spain)*

[b] *Laboratoire de Spectroscopie Moléculaire et Crystalline, Université de Bordeaux I, Bordeaux (France)*

(Received in final form 12 September 1991)

Abstract

A calorimetric study of $[N(CH_3)_4]_2ZnBr_4$ is presented. This compound exhibits a second-order phase transition at 287.20 ± 0.12 K from a high-temperature orthorhombic phase (space group *Pnma*) to a monoclinic ferroelastic phase (space group $P2_1/a$). Specific heat measurements were carried out by automatic adiabatic calorimetry from 170 to 370 K, and the value obtained for the phase transition entropy was $\Delta S = 1.95 \pm 0.1R$ (where R is the ideal gas constant). A simple phenomenological model is found to describe the specific heat below T_c. The experimental set-up and procedure are also described.

INTRODUCTION

Tetramethylammonium tetrabromozincate (TMATB-Zn) belongs to the well-known family of $[N(CH_3)_4]_2MX_4$ crystals (X = halogen and M = Zn, Co, Fe, Mn, etc.). The chlorine derivatives of this family have been extensively investigated in recent years due to their rich variety of phases (incommensurate, ferroelectric, ferroelastic, etc.) [1,2]. However, the bromometallic compounds (M = Zn, Co and Mn) undergo only a second-order phase transition near room temperature from the normal (*Pnma*) to the low temperature ferroeleastic phase ($P2_1/a$) [3]. Several papers on the thermodynamics of the phase transition sequences of these interesting crystals have been published by our group [4,5]. Here we present the

---

Correspondence to: M. Couzi, Laboratoire de Spectroscopie Moléculaire et Crystalline, Université de Bordeaux I, Bordeaux, France.

[1] Presented at the 12th National Conference on Calorimetry and Thermal Analysis, Bari, Italy, 11–13 December 1990.

preliminary results concerning the phase transition at 287.20 ± 0.12 K of TMATB-Zn provided by automatic adiabatic calorimetry as part of a more extensive study using other techniques [6].

Unpublished inprovements of the calorimeter system used in these measurements, including the various experimental procedures available and the automatization of the equipment, are also described.

EXPERIMENTAL

With few alterations concerning the adiabatic control and programmable systems, the design of the calorimeter follows that described by Westrum et al. [7] for solid samples in the low temperature range and was briefly described in ref. 8. Although manually operated in the past, its features have been improved by full automatization of the system control, data acquisition and data processing [9]. In this paragraph, we describe the recently incorporated features of our experimental set-up successfully used in the present measurements.

Calorimeter vessel

A new vacuum-tight calorimeter vessel has been employed for the specific heat measurements. It is a gold-plated copper cylinder with a volume capacity of 40 cm^3 and wall thickness of 0.3 mm. The main difference with respect to that described in ref. 7 is suppression of the copper vanes inside the vessel commonly used to improve thermal conduction across the powder sample. In our case, heat is basically dissipated by the low-pressure He gas (about 0.013 atm) filling the holder. No significant increase of the equilibrium rates was observed. As usual [7], both the heater and the platinum resistance thermometer are located near the cylindrical axis of the vessel to ensure symmetrical heat dissipation and a reliable equilibrium temperature value. The calorimeter was carefully calibrated from 50 to 370 K in 1 K steps. A least squares fitting to a high-degree polynomial provides the vessel heat capacity at every temperature; its value at 300 K is 18.54 J K^{-1}.

Temperature measurement

A 25 Ω platinum resistance thermometer (Leeds and Northrup 1722211) calibrated from 13 to 372 K with an accuracy of 1 mK (K.O.L., Leyden) is placed inside the calorimetric vessel. The actual resistance is measured by an 8 1/2 digit DVM, HP3458A (10 μΩ resolution, 20 ppm accuracy), used exclusively for this purpose, in order to avoid both the thermal e.m.f.s commonly present in multiplexor systems and the transient signals related to switching of the measuring current. The small amount of heat generated in the thermometer due to this current (1 mA), together with other thermal leaks of the calorimetric vessel, is offset by the usual temperature drift correction, as described for example by Westrum et al. [7].

Every temperature assignment is determined by the use of a mean resistance value obtained from a series of five consecutive measurements with the voltmeter operating at the highest resolution. The final temperature value is calculated by the IPTS 1968 (T_{68}) conversion table and from the thermometer specific calibration data. This procedure provides better than 1 mK accuracy. The final result is assigned to the mean time of the measuring interval (about 12 s). This subroutine operates continuously during the equilibrium periods and also in the thermogram technique (see below).

Adiabatic control

The parts of the adiabatic shield (top, side and bottom) to which thermocouples are attached are independently controlled by three PID analog amplifiers. An additional heating current, whose value depends on the temperature range, is used to improve the PID functions. Its value is automatically switched between two prefixed levels for the equilibrium and heating periods, respectively. The temperature imbalances between the shield parts and the calorimeter vessel are monitored by analog voltmeters and also registered by a digital voltmeter to be finally recorded. The temperature is regulated to better than 1 mK.

Power measurements

A heating current up to 40 mA is supplied to the 300 Ω constantan heater by a programable DA converter with better than 20 μA stability. During the heating periods, the heating power (typically 0.1–0.2 W) is determined every 20 s by measuring the voltage across the heater and the current through a 100 Ω standard resistance. Both signals are taken through a multiplexor to a 5 1/2 digital voltmeter. The power data are finally integrated over the heating period to obtain the total energy input.

Experimental procedure

The best accuracy of the specific heat measurements is reached when the system operates in the discontinuous heating or pulse technique. The calibrated accuracy of this experimental set-up was established by C_p measurements on α-Al_2O_3 NBS sample and is better than 0.1% in the whole operating temperature range (50–370 K). The new calibration results are similar to those obtained with the manually operated calorimeter [8]. Although the pulse technique is known to be the most accurate for specific heat measurements where solid–solid phase transitions are present, some of its intrinsic disadvantages cannot be easily avoided. The major limitation lies in the significant temperature increments needed in each heat pulse. Increments of 0.5 K are considered as the lowest limit for accuracy. Smaller steps lead to noticeable dispersion of the experimental points, mainly due to the resolution of our thermometer system (1 mK). This reduces the number of points per fixed temperature range in each series of measurements, and makes it difficult to reach a better resolution of the specific heat curve around the phase transition temperatures, just where it is required. Although other calorimetric methods, such as a.c. calorimetry, are not affected by this shortcoming, the low rate continuous heating–cooling technique [10] (thermograms), which can also be used in our experimental system, provides a much more detailed shape of the specific heat curve in the temperature intervals of interest. Heating rates as low as 0.1 K h^{-1} avoid the presence of high thermal gradients in the sample. This has allowed us to study phase transitions with very low enthalpy changes [11] that cannot otherwise be detected.

Sample

Single crystals of $[N(CH_3)_2]_4ZnBr_4$ were easily obtained from stoichiometric amounts of $N(CH_3)_4Br$ and $ZnBr_2$ in a HBr solution (pH about 2). After two additional crystallizations, the best crystals were kept for other experiments, while the lower quality ones were used for the calorimetric measurements after powdering. Chemical analyses have shown the following percentages (with the theoretical values in parentheses): C, 18.10 (18.01); H, 4.71 (4.54); N, 5.11 (5.25); Br, 59.99 (59.94).

X-Ray powder diffraction has been also used to confirm the crystallographic quality of the sample. The best assignment of the various reflections has been attained with the following values for the cell constants: $a = 12.62$ Å, $b = 16.05$ Å, $c = 9.18$ Å, in good agreement with previous results [2,12].

RESULTS

32.4308 g of a TMATB-Zn powder sample were employed for the calorimetric measurements. The pulse technique was used from 180 to 350 K with about 1 K temperature steps. In addition, two independent heating thermograms were made in the range 230–320 K with two heating rates: 1.5 and 0.6 K h^{-1}.

A final low-rate cooling thermogram (about 0.5 K h^{-1}) around the phase transition temperature did not show any noticeable thermal hysteresis of T_c, in agreement with the second-order character assigned to the phase transition [3,13].

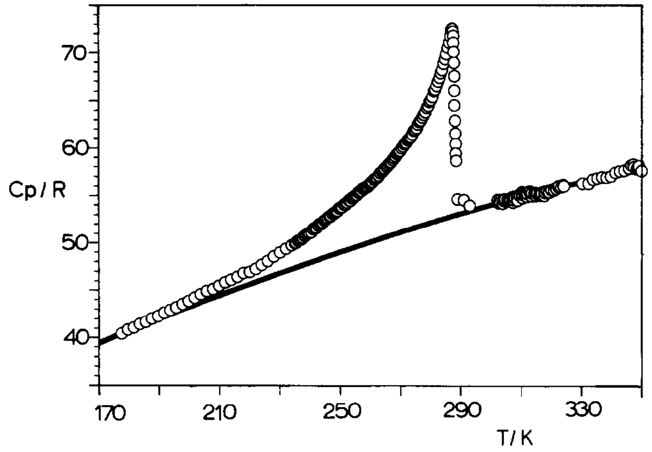

Fig. 1. The specific heat of $[N(CH_3)_4]_2ZnBr_4$ around the ferroparaelastic phase transition. The baseline (continuous line) has been established from both the harmonic and anharmonic contributions to the specific heat, from Raman, IR, elastic constants and thermal expansion data.

As usual for this kind of phase transition, the associated specific heat anomaly measured in TMATB-Zn spreads over a very wide temperature range. As shown in preliminary DSC measurements, the phase transition starts at around 180–200 K [13], about 100 K below the transition temperature. The experimental results obtained by adiabatic calorimetry are represented in Fig. 1, and the specific heat values are shown in Table 1.

As this type of behaviour usually makes it difficult to calculate the thermodynamic functions associated with the phase transition itself, we have estimated independently the harmonic and anharmonic contributions to the specific heat, following the procedures used in previous works [14]. It can be shown that above 150 K the behaviour of the harmonic specific heat in the compounds belonging to this family depends mainly on the relatively high frequencies (above 200 cm^{-1}) associated with the internal modes of the organic and inorganic tetrahedra. The external modes, with much lower frequencies, contribute to the specific heat with practically saturated values above 150 K. From the available Raman and IR data [13], we have constructed the harmonic specific heat from 180 to 350 K by means of Einstein functions. As also shown in refs. 13 and 14, the anharmonic contribution to the specific heat can be calculated from the elastic constants and thermal expansion data.

These results have permitted us to calculate a specific heat baseline which fits the experimental points on both sides of the transition anomaly quite well (see Fig. 1). A careful estimation of the various sources of error, mainly due to the incomplete information of the low-frequency external modes, and the use of the Nernst–Lindemann law [15] for the anharmonic specific heat limit the accuracy of the calculated thermodynamic functions

TABLE 1

Experimental specific heats of $[N(CH_3)_4]_2ZnBr_4$

T (K)	C_p (R)	T (K)	C_p (R)	T (K)	C_p (R)	T (K)	C_p (R)	T (K)	C_p (R)
191.684	42.59	245.935	52.64	267.848	58.96	287.110	72.49	311.813	54.92
193.699	42.90	246.474	52.83	268.349	59.16	287.199	72.50	311.943	55.22
195.716	43.15	247.013	52.87	268.850	59.39	287.287	72.47	312.740	55.47
197.730	43.53	247.551	53.07	269.349	59.56	287.375	72.21	313.207	55.26
199.744	43.84	248.089	53.13	269.848	59.71	287.460	71.76	313.309	54.97
201.761	44.20	248.626	53.29	270.346	59.99	287.552	71.03	313.541	55.31
203.776	44.57	249.161	53.41	270.842	60.20	287.641	70.11	314.343	55.26
205.795	44.90	249.696	53.67	271.338	60.44	287.730	68.93	314.695	55.31
207.812	45.11	250.228	53.72	271.832	60.60	287.822	67.56	314.802	55.03
209.821	45.48	250.762	53.80	272.324	60.86	287.914	66.06	315.141	55.26
211.832	45.85	251.293	54.08	272.817	61.02	288.009	64.49	315.940	55.07
213.852	46.11	251.824	54.09	273.307	61.17	288.104	62.92	316.184	55.32
215.868	46.42	252.355	54.26	273.798	61.45	288.201	61.59	316.291	55.11
217.880	46.82	252.884	54.54	274.286	61.83	288.300	60.46	316.739	55.20
219.987	46.95	253.411	54.49	274.774	61.93	288.399	59.45	317.541	55.05
222.007	47.28	253.940	54.76	275.261	62.13	288.500	58.67	317.674	55.45
223.978	47.70	254.465	54.83	275.745	62.52	288.979	54.64	317.780	55.32
226.011	48.10	254.992	55.02	276.229	62.79	291.104	54.55	318.344	55.50
228.003	48.57	255.516	55.11	276.712	62.98	293.111	53.97	319.151	55.42
229.980	49.00	256.040	55.35	277.193	63.29	302.315	54.59	319.275	55.41
231.979	49.40	256.563	55.46	277.673	63.55	302.718	54.24	319.958	55.63
234.004	49.75	257.085	55.51	278.152	63.81	302.857	54.51	320.760	55.70
235.048	49.94	257.607	55.72	278.629	64.24	303.118	54.27	320.773	55.60
235.495	50.05	258.127	55.79	279.105	64.46	303.919	54.20	321.564	55.72
236.053	50.26	258.647	55.92	279.579	64.90	304.363	54.45	322.268	55.95
236.609	50.30	259.166	55.97	280.052	65.10	304.718	54.67	322.364	56.01
237.166	50.40	259.685	56.18	280.524	65.41	305.526	54.58	323.168	55.96
237.721	50.57	260.202	56.34	280.994	66.01	305.860	54.49	323.770	56.13
238.275	50.75	260.719	56.44	281.461	66.20	306.334	54.61	323.971	56.02
238.828	50.89	261.235	56.71	281.929	66.56	307.135	54.86	330.196	56.31
239.382	50.98	261.749	56.83	282.394	67.00	307.210	54.32	332.191	56.31
239.932	51.06	262.262	56.90	282.856	67.41	307.343	54.61	333.690	56.72
240.484	51.14	262.776	57.09	283.319	67.90	307.939	54.79	335.191	56.86
241.034	51.47	263.287	57.36	283.778	68.21	308.712	54.76	336.693	56.95
241.581	51.56	263.798	57.51	284.236	68.86	308.742	54.98	338.188	56.94
242.128	51.63	264.307	57.66	284.691	69.33	308.832	54.52	339.682	57.05
242.675	51.87	264.816	57.83	285.145	69.88	309.542	55.05	341.174	57.46
243.220	52.04	265.324	58.04	285.595	70.54	310.200	55.40	342.679	57.59
243.765	52.01	265.831	58.22	286.044	71.08	310.322	54.78	344.182	57.67
244.309	52.17	266.336	58.42	286.491	71.71	310.344	55.16	345.672	57.94
244.852	52.38	266.841	58.53	286.934	72.43	311.144	55.19	346.442	58.25
245.394	52.49	267.345	58.77	287.023	72.47	311.706	55.15	347.167	58.32

of the phase transition to 5%. These values are, $\Delta H/R = 490 \pm 30$ K and $\Delta S/R = 1.95 \pm 0.1$.

These results are in good agreement with the order–disorder character

TABLE 2

The phase transition Gibbs energy of $[N(CH_3)_4]_{2p}ZnBr_4$

T (K)	$\Delta G/R$ (K)	T (K)	$\Delta G/R$ (K)	T (K)	$\Delta G/R$ (K)	T (K)	$\Delta G/R$ (K)
249.161	−31.39	259.685	−18.62	269.848	−8.65	279.579	−2.22
249.696	−30.72	260.202	−18.00	270.346	−8.29	280.052	−2.00
250.228	−29.99	260.719	−17.45	270.842	−7.89	280.524	−1.79
250.762	−29.32	261.235	−16.90	271.338	−7.50	280.994	−1.60
251.293	−28.66	261.749	−16.34	271.832	−7.11	281.461	−1.40
251.824	−27.92	262.262	−15.91	272.324	−6.71	281.929	−1.23
252.355	−27.25	262.776	−15.29	272.817	−6.37	282.394	−1.05
252.884	−26.59	263.287	−15.24	273.307	−5.97	282.856	−0.90
253.411	−25.93	263.798	−14.80	273.798	−5.63	283.319	−0.75
253.940	−25.33	264.307	−13.76	274.286	−5.29	283.778	−0.59
254.465	−24.67	264.816	−13.26	274.774	−5.04	284.236	−0.50
254.992	−24.00	265.324	−12.77	275.261	−4.66	284.691	−0.40
255.516	−23.41	265.831	−12.28	275.745	−4.36	285.145	−0.30
256.040	−22.80	266.336	−11.79	276.229	−4.07	285.595	−0.24
256.563	−22.19	266.841	−11.30	276.712	−3.77	286.044	−0.17
257.085	−21.57	267.345	−10.87	277.193	−3.48	286.491	−0.09
257.607	−20.96	267.848	−10.43	277.673	−3.22	286.934	−0.07
258.127	−20.33	268.349	−9.95	278.152	−2.96	287.023	−0.02
258.647	−19.79	268.850	−9.52	278.629	−2.70	287.110	0.00
259.166	−19.17	269.349	−9.08	279.105	−2.44	287.199	0.00

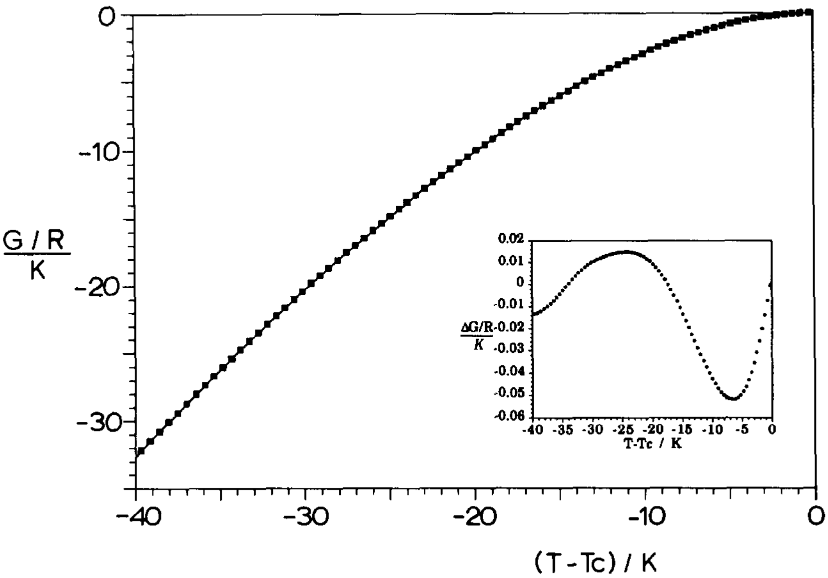

Fig. 2. The experimental Gibbs energy (points) is compared with the phenomenological function eqn. (1). Deviations are shown in the insert. The values found for the coefficients are $\alpha = 1$, $\beta = 7.3074$, $\gamma = 1.0229$, $\delta = 0.7079$. Gibbs energy is given in units of R.

assigned to the phase transition [13,16]. A comparative discussion of the thermodynamic behaviour in the various members of the family will be published elsewhere [13].

In addition, it has been found that the Landau theory for second-order phase transitions describes the thermodynamic behaviour of this crystal below the transition temperature quite well. For this purpose, we have used the well-known Gibbs energy expansion in powers of the order parameter

$$G = G_0 + \tfrac{1}{2}\alpha Q^2 + \tfrac{1}{4}\beta Q^4 + \tfrac{1}{6}\gamma Q^6 + \tfrac{1}{8}\delta Q^8 + \ldots \qquad (1)$$

where Q is the order parameter.

The use of this function together with the experimental values of the Gibbs energy (shown in Table 2) have permitted an empirical fitting of the phenomenological coefficients. The results obtained are shown in Fig. 2. It should be noted that the fit is excellent in the immediate vicinity of the phase transition temperature $|T - T_c| \approx 0.1$ K. This seems to rule out appreciable contributions due to critical fluctuations in the near proximity of the transition temperature, a common fact observed where very-long-range forces associated with ferroelastic ordering are present [17].

The general procedure described above allows accurate studies of the thermodynamics of the second-order phase transition when only incomplete experimental spectroscopic and elastic data are available.

ACKNOWLEDGEMENTS

This work has been supported by the Eusko Jaurlaritza/Gobierno Vasco under project No 0633100012/88 and by the Euskal Herriko Unibertsitatea/Universidad del Pais Vasco under project No. 662-91.

REFERENCES

1 H. Shimizu, N. Abe, N. Kokubo, S. Fujimoto, T. Yamaguchi and S. Sawada. Solid State Commun., 34 (1980) 363.
2 K. Gesi. Ferroelectrics, 66 (1986) 269.
3 K. Gesi. J. Phys. Soc. Jpn., 51 (1982) 203.
4 A. López-Echarri, M.J. Tello, C. Socias and J. Herreros, J. Phys. C, 18 (1985) 2631.
5 A. López-Echarri, I. Ruiz-Larrea and M.J. Tello, Phys. Status Solidi B, 154 (1989) 143.
6 T. Breczewski, A. Gómez-Cuevas, E.H. Bocanegra, J.M. Igartua and A.R. Arnaiz, Solid State Commun., submitted.
7 E.F. Westrum, Jr., G.T. Furukawa and J.P. McCullough, in J.P. McCullough and D.W. Scott (Eds.), Experimental Thermodynamics: Calorimetry of Non-Reacting Systems, Vol. 1, Butterworths, London, 1968, Chapter 5.
8 A. López-Echarri and M.J. Tello, J. Phys. D, 14 (1981) 71.
9 J. Zubillaga, A. López-Echarri and M.J. Tello, Thermochim. Acta, 92 (1985) 283.
10 I. Ruiz-Larrea, A. López-Echarri and M.J. Tello, J. Phys. C, 14 (1981) 3171.
11 J. Zubillaga, A. López-Echarri and M.J. Tello, J. Phys. C, 21 (1988) 4417.

12 P. Troulean, J. Lefebvre and P. Derollez. Acta Crystallogr., Sect. C, 40 (1984) 386.
13 J.M. Igartua, I. Ruiz-Larrea, M. Couzi, A. López-Echarri and T. Breczewski, Phys. Status. Solidi. B, 168 (1991) 67.
14 A. Lóez-Echarri, I. Ruiz-Larrea and M.J. Tello, J. Phys. Condens. Mater., 2 (1990) 513.
15 E.S.R. Gopal, Specific Heat at Low Temperatures, Heywood Books, London, 1966.
16 R. Perret, Y. Beaucamps, G. Godefroy, P. Muralt, M. Ehresperger, H. Arend and D. Altermatt, J. Phys. Soc. Jpn., 52 (1983) 2523.
17 L.T. Cheng and K.A. Nelson, Phys. Rev. B, 37 (1988) 3603.